

TRIUMF	4004 WESBROOK MALL, VANCOUVER, B.C. V6T 2A3		PAGE 1
DESIGN NOTE	NAME D. Kaltchev	DATE March 23,2007	FILE NO. TRI-DN-07-9

SUBJECT

On beam-beam resonances observed in LHC tracking



Abstract

The Lie algebraic method is used to construct the nonresonant Courant-Snyder invariant in the presence of beam-beam interactions occurring at several Interaction Points (IP). The number of IP-s is arbitrary, but we assume round beams at all IP-s and only head-on collisions. Tracking evidence is presented to illustrate that the invariant is indeed preserved for a wide range of parameters, except near resonances. By taking two IP-s and the parameters of LHC at collision energy, we explain two dips in dynamic aperture observed previously in Sixtrack simulations. We further derive the condition for a resonance to be canceled – the betatron phase of the second IP must be a multiple of 90 degrees. Resonances of order divisible by four cannot be canceled in this way. The above analytical results are confirmed on a simple 4D tracking model.

On beam-beam resonances observed in LHC tracking

D. Kaltchev

November 12, 2008

1 Introduction

The goals of this note are:

1. To explain two areas of low dynamic aperture (resonance dips) observed previously in long-term tracking performed with Sixtrack [1]. These dips were found to appear consistently on the tune-scan curve, i.e. the curve representing dependence of dynamic aperture on ring tune. They are positioned on both sides of the LHC working point at collision energy (Figure 1).
2. By taking the subject a little further, we derive an expression for the horizontal betatronic invariant in presence of an **arbitrary number of head-on collision points**. Tracking tests performed on a simple model demonstrate that the invariant is indeed preserved for a wide range of parameters, except near resonances.

We have studied the invariant 2) in conditions close to the ones taken in 1). There are only two IP-s, Atlas and CMS of the LHC. The resonant tunes (for which the betatronic invariant diverges) depend only on the phase of the second IP (CMS). If this phase is taken to be arbitrary, as in 1) then indeed two, and only two, resonance tunes exist at locations that explain very well the Sixtrack results. We derive the condition for resonance cancellation to find that one of the resonance dips would disappear if the above phase is set to $\pm\pi/2$. We also show that resonances of order divisible by four (including the second observed resonance) can not be canceled in this way.

The analytical formula for the invariant in 2) is derived via Lie algebraic methods. It should be noted that such model: does not predict where the nonlinear tune shift will pull the particle out of resonance; it does not include the crossing angle (only even order resonances excited), and the synchrotron satellites are not included.

Nevertheless, there are strong arguments that the resonances are correctly identified and explained:

- 1) the dynamic aperture dips are predominantly in the horizontal plane – 1D theory seems sufficient;
- 2) these dips disappear if we remove the head-on collisions, keeping only the parasitics and the crossing angle.
- 3) a 2D plot of resonances around the working point 64.31, 59.32 shows only these resonances

Everywhere in this paper, the LHC beam parameters at collision were used: proton radius $r_p = 1.53469810^{-18}$ m; number of protons per bunch $N_p = 1.15 \cdot 10^{11}$; beam gamma: $\gamma = 7462.7$; normalized emittance $\epsilon \times \gamma = 3.7510^{-6}$ m rad; beam-beam parameter $B = \frac{N_p r_p}{\gamma} = 2.262110^{-11}$; incoherent beam-beam tune shift per interaction point (IP): $\xi = \frac{N_p r_p \beta}{4\pi \gamma \sigma^2} = 0.003582$.

In [2], a similar tracking model as in this paper has been used and resonances identified by the growth of particle amplitude.

2 Resonances $Q_x = 4/13$ and $Q_x = 5/16$

2.1 Observation

The 10^6 -turn tracking carried out in [1] shows two resonance dips positioned in vicinity of the nominal LHC working point $Q_x = 64.31$, $Q_y = 64.32$, see Figure 1.

The tracking conditions are: beam-beam interactions only (no other errors); head-on and parasitic collisions at IP1 and IP5 with β^* value 0.55 m and crossing angle 0.2 mrad. The unperturbed tune Q_x is varied within 64.3–64.33. The vertical one is chosen with a constant tune split $Q_y - Q_x = 0.01$. Figuratively, the working point moves along the diagonal in tune space (step 0.0005). Here “angle” stands for $\arctan(x_{ini}/y_{ini})$, so that its zero value corresponds to a particle launched in the horizontal plane.

It was found that these dips: 1) occur for particles launched near the horizontal plane (by varying the initial coordinates x_{ini} and y_{ini}); 2) are caused by beam-beam resonances (switching off/on all other errors); 3) are caused by head-on beam-beam collisions (by switching off parasitics).

2.2 Explanation with the analytical formula (17).

To explain the resonance dips seen on Figure 1, on Figure 2 we plot the expression (17) where the position of peaks is to be compared with the dips

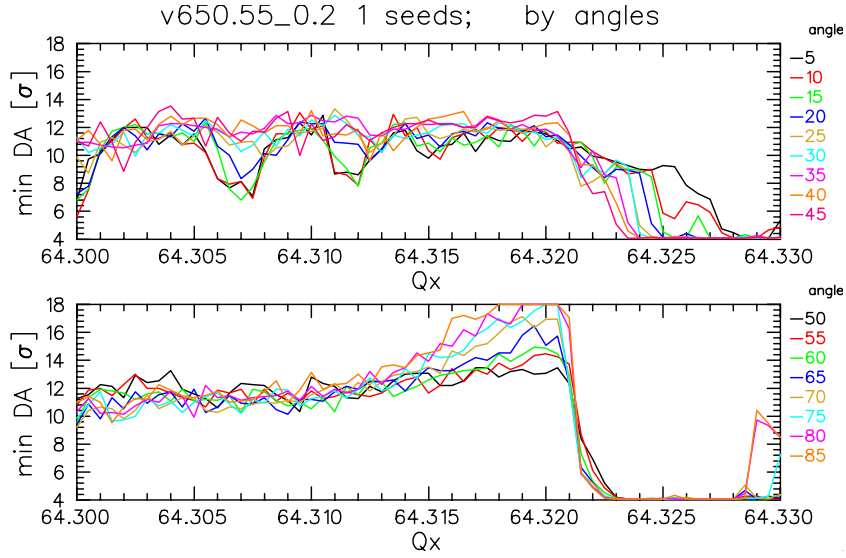


Figure 1: Minimum dynamic aperture and two dips on both sides of the nominal working point near $Q_x = 4/13 = 0.3077$ and $Q_x = 5/16 = 0.3125$ get eps

on Figure 1. The amplitude at which the resonances become dominant can be deduced by looking at Figure 4.

3 Horizontal betatronic invariant for an arbitrary number of IPs

3.1 One IP

By following mainly [3], the one-turn Lie map transforming the weak beam in horizontal phase space (x, p_x) is:

$$e^{if_2} e^{iF} = e^{ih}, \quad (1)$$

where

$$F = \int_0^x dx' \frac{2B}{x'} \left[1 - \exp\left(\frac{x'^2}{2\sigma^2}\right) \right] = \sum_{n=-\infty}^{\infty} c_n(I) e^{in\phi} \quad (2)$$

$$I = \frac{\beta^* A}{\sigma^2} = \frac{A}{\epsilon}. \quad (3)$$

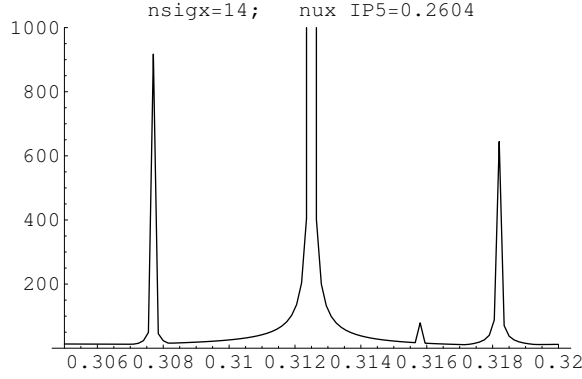


Figure 2: Expression (17) plotted as a function of μ . The second IP phase $\mu_1 = 2\pi\nu_{IP5}$ is taken as in Sixtrack tracking: $\nu_{IP5} = 0.2604$. [get eps](#)

Here $B = \frac{N_p r_p}{\gamma}$ and A and ϕ are action-angle variables defined by:

$$x = \sqrt{2A\beta^*} \sin \phi; \quad p_x = \sqrt{2A/\beta^*} \cos \phi.$$

The Fourier coefficients c_n can be expressed [3] via the Bessel I-functions \mathcal{I}_k :

$$c_n(I) = \left\{ \begin{array}{ll} \text{n odd} & 0, \\ \text{n = 0} & B \int_0^{I/2} \frac{1}{a} [1 - e^{-a} \mathcal{I}_0(a)] da, \\ \text{n even} & -B \int_0^{I/2} \frac{e^{-a}}{a} \mathcal{I}_{n/2}(a) da. \end{array} \right\}. \quad (4)$$

Our goal is to find the effective Hamiltonian, i.e. the function $h(A, \phi)$ to first order in the perturbation parameter B , or F . The Lie operator representing the beam-beam map is e^{iF} , while e^{if_2} with

$$: f_2 : := -\mu A \quad (5)$$

acts in the same way as the linear-ring matrix $R = R(\nu, \beta^*)$, where $\nu \equiv Q_x = \mu/(2\pi)$ is the ring tune. A basic property of $: f_2 :$ is to operate in a very simple way on functions of A , on eigen-vectors, or functions of eigen-vectors. For example:

$$\begin{aligned} : f_2 : c_n(I) &= 0, \\ : f_2 : e^{in\phi} &= i n \mu e^{in\phi}. \end{aligned} \quad (6)$$

Further, for an arbitrary function G , we have:

$$G(: f_2 :) e^{in\phi} = G(in\mu) e^{in\phi}, \quad (7)$$

which is to be understood as infinite series of Lie brackets. To first order in F one has:

$$:h: \approx -:f_2: + \frac{:f_2:}{1 - e^{:f_2:}} F = -:f_2: + \frac{:f_2:}{1 - e^{:f_2:}} \sum_{n=-\infty}^{\infty} c_n(I) e^{in\phi}, \quad (8)$$

where the first approximate equality follows from the BCH theorem. By using (5), (6) and (7):

$$h \approx -\mu A + \sum_{n=-\infty}^{\infty} c_n(I) \frac{in\mu}{1 - e^{-in\mu}} e^{in\phi} = -\mu A + \sum_{n=-\infty}^{\infty} c_n(I) \frac{n\mu/2}{\sin n\mu/2} e^{in(\phi+\mu/2)} \quad (9)$$

This expression (it can be found as (9.738) in [3]) is real since c_n are non-zero only for even n . For small perturbations and far from resonances, particle coordinates in phase space are restricted on the Poincare surface of section:

$$h = const. \quad (10)$$

3.2 Two and more IPs

In case of only two IPs being present, each delivers a Lie kick $e^{:F^{(1)}:}$, or $e^{:F^{(2)}:}$. Let the operator $e^{:f_2:}$ still represent the linear ring, but now there are two additional linear operators describing transport between the kicks: $e^{:f_2^{(1)}:}$ and $e^{:f_2^{(2)}:}$. As it is usually done, we will first write the expression for the one-turn map and then use similarity rules to transform all linear operators to the end of the ring:

$$\begin{aligned} & e^{:f_2^{(1)}:} :e^{:F^{(1)}:} :e^{:f_2^{(2)}:} :e^{:F^{(2)}:} = \\ & = e^{:f_2^{(1)}:} :e^{:F^{(1)}:} :e^{:-f_2^{(1)}:} :e^{:f_2^{(1)}:} :e^{:f_2^{(2)}:} :e^{:F^{(2)}:} = \\ & = e^{:f_2^{(1)}:} :e^{:F^{(1)}:} :e^{:-f_2^{(1)}:} :e^{:f_2:} :e^{:F^{(2)}:} :e^{:-f_2:} :e^{:f_2:} = \\ & = e^{:e^{:-f_2^{(1)}:} :F^{(1)}:} :e^{:e^{:-f_2:} :F^{(2)}:} :e^{:f_2:} = \\ & = e^{:h:} \end{aligned} \quad (11)$$

Here f_2 is given by (5), while $:f_2^{(1)}: = -\mu_1 A$, with μ_1 being the betatron phase of the first IP. The second IP is at phase zero (or μ), so only f_2 and $f_2^{(1)}$ appear in the final expression (11) while $f_2^{(2)}$ does not.

From the properties of eigen-vectors it follows that when an operator $e^{:f_2^{(1)}:}$ acts on $F^{(1)}$, it commutes with $c_n(I)$ and only shifts the phase:

$$e^{:f_2^{(1)}:} e^{in\phi} = e^{in\mu_1} e^{in\phi} = e^{in(\mu_1+\phi)}. \quad (12)$$

The same is true for f_2 . The two-IP map (11) is then obtained via two simple replacements:

$$e^{:h:} = e^{:F^{(1)}|_{\phi \rightarrow \phi + \mu_1}:} e^{:F|_{\phi \rightarrow \phi + \mu}:} e^{:f_2:}. \quad (13)$$

By neglecting the cross-terms of BCH, in (13) we simply add the exponent factors. The total beam-beam kick equivalent to the action of two IPs, but applied at ring entrance, becomes:

$$e^{:F^{(1)}|_{\phi \rightarrow \phi + \mu_1} + F|_{\phi \rightarrow \phi + \mu}:}.$$

This combined kick is followed by the same linear matrix as in (8), only the order is reversed – ring entrance rather than end. This just changes the sign of f_2 so one can simply replace in (8) F by $F^{(1)}|_{\phi \rightarrow \phi + \mu_1} + F|_{\phi \rightarrow \phi + \mu}$.

The invariant h , written for one or two IPs, is:

$$\begin{aligned} h_{one} &= -\mu A + \tilde{h}(\mu, 0), \\ h_{two} &= -\mu A + \tilde{h}(\mu, 0) + \tilde{h}(\mu, \mu_1) \\ \text{where } \tilde{h}(\mu, \tilde{\mu}) &= \sum_{n=-\infty}^{\infty} \frac{n\mu}{2\sin(n\mu/2)} c_n(I) e^{in(\phi + \tilde{\mu} + \mu/2)}. \end{aligned} \quad (14)$$

Only even n contribute, positive or negative, since $c_n = 0$ if n is odd. We have introduced an auxiliary function \tilde{h} . The formula for the invariant **for an arbitrary number of head-on collision points** can now be deduced from (14). The case of off-set (parasitic) collisions can also be included.

The invariant surface is defined by (10). For numerical calculations, we divide both sides of (14) by $\mu\epsilon$ and will plot $\pi/2 + \phi$ instead of ϕ . Only the oscillating with ϕ parts enter the expressions for the invariant – the constant part is subtracted. For an arbitrary number of interaction points, located at betatron phases 0 (or μ), μ_1, μ_2, \dots , the analytical invariant I as a function of the initial $I_{x,0}$ and phase ϕ , is:

$$\begin{aligned} I_{one}^{analyt} &= I_{x,0} + \frac{1}{\epsilon} \left[\tilde{h}(\phi, 0) - \tilde{h}(0, 0) \right] \\ I_{two}^{analyt} &= I_{one}^{analyt} + \frac{1}{\epsilon} \left[\tilde{h}(\phi, -\mu_1) - \tilde{h}(0, -\mu_1) \right] \\ I_{three}^{analyt} &= I_{two}^{analyt} + \frac{1}{\epsilon} \left[\tilde{h}(\phi, -\mu_2) - \tilde{h}(0, -\mu_2) \right] \\ &\dots \\ \text{where } \tilde{h}(\phi, \tilde{\mu}) &= \sum_{n=-N}^N \frac{n}{2\sin(n\mu/2)} c_n(I_{x,0}) e^{in(\pi/2 + \phi + \tilde{\mu} + \mu/2)} \end{aligned} \quad (15)$$

We take a number of harmonics $N = 40$ (this is the maximum order of resonance that can be observed).

3.3 Phase difference $\pi/2$ between two IPs and cancellation of some resonances

If there is only one IP, then considering h_{one} in (14), the term with $n=0$ yields, after differentiating it over the action A , the amplitude-dependent tune shift $\Delta\nu$:

$$2\pi\Delta\nu = -\frac{d}{dA}c_0(I) = -\frac{N_p r_p \beta^*}{2\sigma^2 \gamma} \zeta(I) = 2\pi \xi \zeta(I), \quad (16)$$

where $\zeta(I) = \frac{2}{I} [1 - e^{-I/2} \mathcal{I}_0(I/2)]$ tends to unity for $I \rightarrow 0$.

Of the remaining terms, each contains a denominator $\sin(n\pi\nu)$, where $\nu = \frac{\mu}{2\pi}$ is the ring tune. As ν approaches a resonance $\frac{N}{M}$, where N and M are integers, one term becomes infinite – the one with $n = M$ if M is even, or $n = 2M$ if M is odd.

If there are two IPs, one positioned at zero phase and another at phase μ_1 , then by using the asymmetry $c_{-n}(I) = c_n(I)$, (14) gives:

$$\begin{aligned} h_{two} &= -\mu A + \tilde{h}(\mu, \mu_1) + \tilde{h}(\mu, 0) = \\ &= -\mu A + \sum_{n=-\infty}^{\infty} \frac{n \mu c_n(I)}{2\sin(n\mu/2)} [e^{i n (\phi + \mu/2 + \mu_1)} + e^{i n (\phi + \mu/2)}] = \\ &= -\mu A + 2 c_0(I) + \sum_{n=2,4,\dots}^{\infty} \frac{n \mu c_n(I)}{\sin(n\mu/2)} [\cos n(\phi + \mu/2 + \mu_1) + \cos n(\phi + \mu/2)] = \\ &= -\mu A + 2 c_0(I) + \sum_{n=2,4,\dots}^{\infty} \frac{2 n \mu c_n(I)}{\sin(n\mu/2)} \cos [n(\phi + \mu/2 + \mu_1/2)] \cos(n\mu_1/2) \end{aligned} \quad (17)$$

If the phase advance of the second IP is chosen to be $\mu_1 = \pi/2 \times (\text{integer})$ and n is divisible by 4, then the corresponding n th term is resonant – it becomes infinite as the denominator tends to zero. However the terms with $n = 2 \times (\text{odd integer})$ are finite because the factor $\cos(n\mu_1/2)$ cancels the zero denominator.

We conclude that *choosing a phase advance between the two IP-s equal to $\pi/2 \times (\text{integer})$ cancels those resonances for which n is not divisible by 4*. In particular, if M is an odd number, then the corresponding resonance is canceled. Of the two resonances mentioned in Section 2, $\nu = 4/13$ can be compensated in this way, while $\nu = 5/16$ can not.

Figure 3 is to be compared with Figure 2. It shows that the resonance peak $\nu = 4/13$ disappears for IP5 phases ν_{IP5} equal to 0.06 and 0.25.

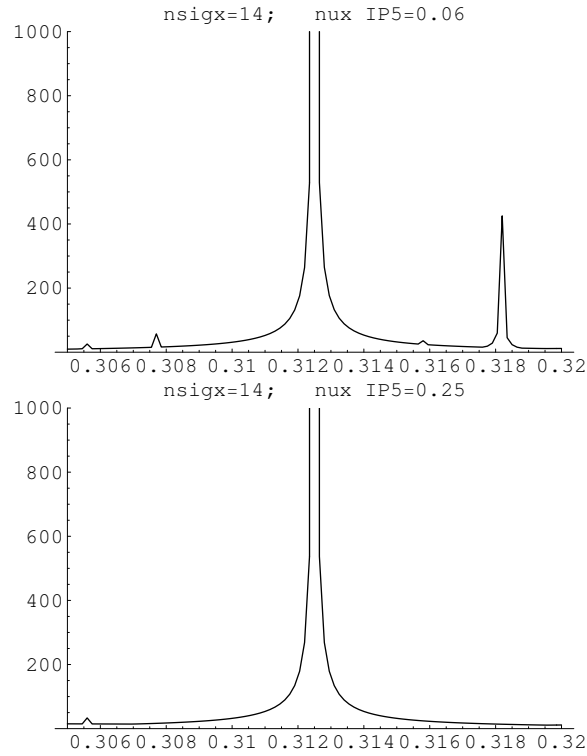


Figure 3: Expression (17) plotted if the IP5 phase is $\pi/2 \times (\text{integer})$. Only the value 0.25 gives complete cancellation, while $0.31 - 0.25 = 0.06$ is not perfect. `get eps get eps`

4 Simple tracking model – verification of the invariant

At each IP (beam-beam kick) the beams are round, i.e. beta-functions and sigmas at IP are equal in both planes and we take: $\beta^* = 0.55 \text{ m}$ $\sigma = \sqrt{\epsilon\beta^*} = 1.66 \cdot 10^{-5} \text{ m}$ for both planes and for both IP-s

A simple tracking model is then constructed in four dimensions. The linear section matrix is $R = R(\nu_x, \nu_y, \beta^*)$ and the numerical map transforming the 4D coordinate vector X through one IP plus one linear section is:

$$R(\nu_x, \nu_y, \beta^*) \cdot (X + \Delta X),$$

where $\Delta X = (0, \Delta p_x, 0, \Delta p_y)$ with

$$\begin{pmatrix} \Delta p_x(x,y) \\ \Delta p_y(x,y) \end{pmatrix} = \frac{2B}{r^2} \left[1 - \exp\left(\frac{r^2}{2\sigma^2}\right) \right] \begin{pmatrix} x \\ y \end{pmatrix}, \quad (18)$$

$$r^2 \equiv x^2 + y^2. \quad (19)$$

For the case of two IP-s, two identical such maps are applied one after another. Iterating the numerical for 2^{10} turns takes several seconds on 1GHz processor.

We choose an initial vector $(x, p_x, y, p_y) = (n_x \sigma_x, 0, n_y \sigma_y, 0)$ and use our simple model to test the invariant (15). The starting number of sigmas n_x is linked to the initial value of I (action divided by emittance) by $I_{x,0} = A\beta^*/\sigma^2 = A/\epsilon = n_x^2/2$ and the same for vertical. The horizontal coordinates (x, p_x) after each turn are used to compute :

$$I_x^{num} = A\beta^*/\sigma^2 = \frac{\beta^*}{2\sigma^2} (x^2/\beta^* + p_x^2\beta^*) \quad (20)$$

and the phase

$$\phi^{num} = \arctan\left(\frac{p_x}{x}\right)$$

This I_x^{num} is to be compared with the result (14) from the perturbation theory.

5 Results

See Figures 5, 6, 7, 8. The numerical model (black dots) and the analytical horizontal invariant (red curve) agree nearly exactly for all meaningful parameters if the tune is not very close to resonance and the number of sigmas is kept below, say, $n_x < 20$. If the particle is launched in or near the horizontal plane: $n_y \approx 0$, then on the plane I_x, ϕ the tracking points – values of the numerical action (20) – lay on the curve I_{one}^{analyt} , or I_{two}^{analyt} . If n_y is of the order of n_x , then far from resonances these points are all inside some area still bordered by the invariant I^{analyt} . The picture changes near resonance: the oscillations of the invariant curve increase and the tracking points deviate from it – diffusion takes place in action space.

A tune scan has been performed to demonstrate the improvement in dynamics: the plot without cancellation is on Fig. 9 – to be compared with Fig. 10 where the IP5 phase set to $\pi/2$

References

- [1] W. Herr, E. McIntosh, F. Schmidt, D. Kaltchev, *Large Scale Beam-beam Simulations for the CERN LHC Using Distributed Computing*, in the Proc. EPAC 2006, Edinburgh, Scotland
- [2] W. Herr, Computer simulation of synchrotron resonances induced by a non-zero crossing angle in the LHC, CERN SL/90-69 (AP) (1990); see zwe.home.cern.ch
- [3] A. Chao, Truncated Power Series Algebra, lectures

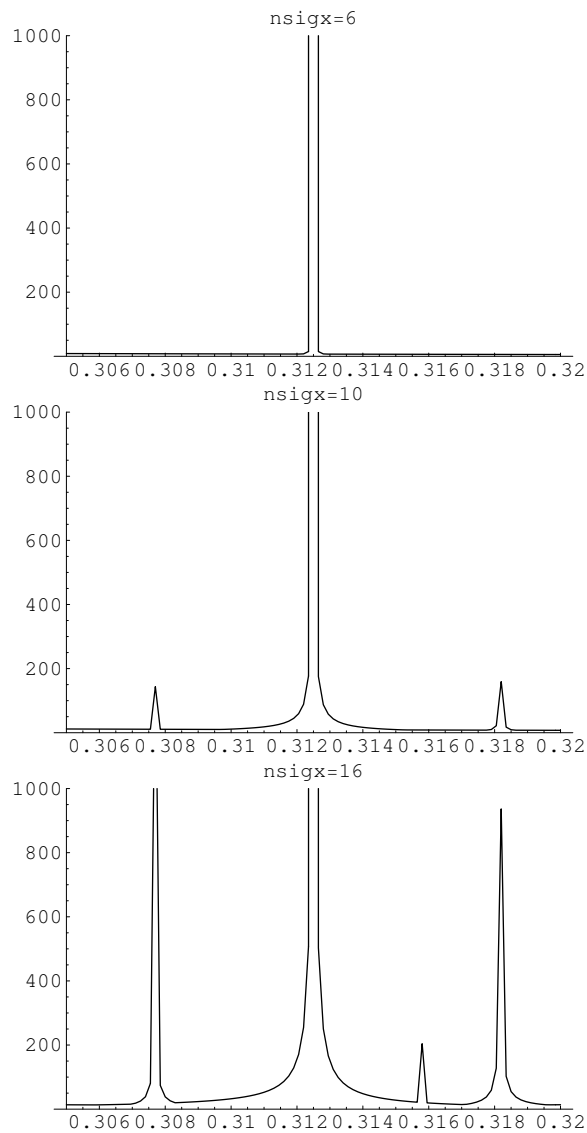


Figure 4: Dependence on initial amplitude for $\mu_{IP5,x} = 0.2604$. `get eps`
`get eps get eps`

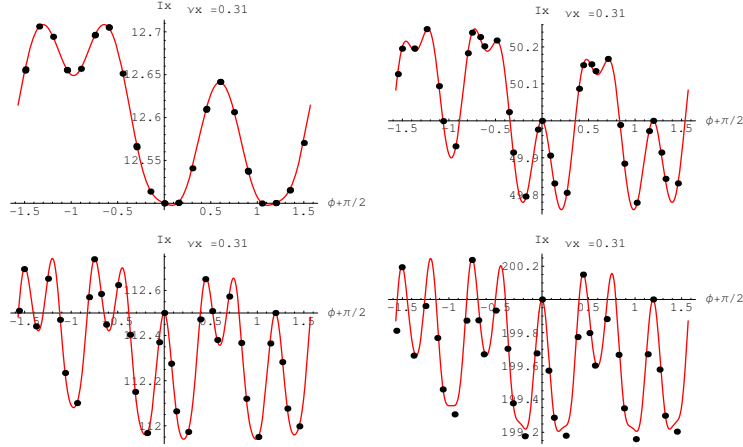


Figure 5: Here start in the horizontal plane $y_{ini} = 0$ and a small number of turns to test the invariant (2^5) . Shown are I_{one}^{analyt} (red) and I^{num} (black) for $Q_x = 0.31$ (far from resonance) and increasing number of sigmas: $n_x = 5, 10, 15$ and 20 ($I_{x,0} = 12.5, 50, 112.5$ and 200) [get eps get eps get eps get eps](#)

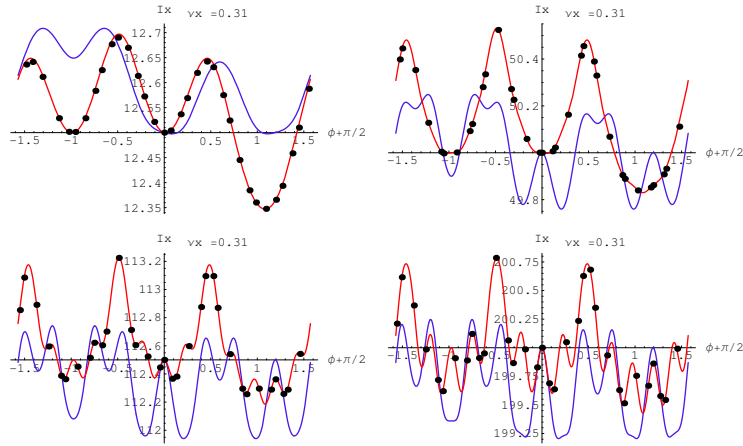


Figure 6: Same parameters as on the previous Figure 5 but with two IP-s. Shown are I_{one}^{analyt} (blue) I_{two}^{analyt} (red) and I^{num} (black). [get eps get eps get eps get eps](#)

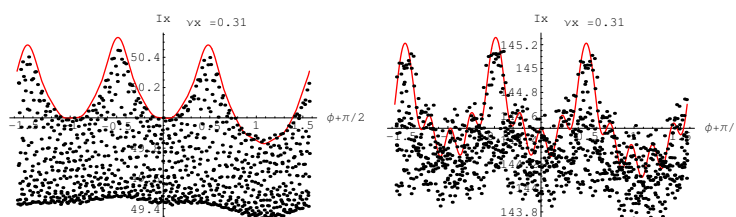


Figure 7: A nonzero y_{ini} , 2^{10} turns, in case of two IP-s. Left: $n_x = 10$; Right $n_x = 17$. Show are I_{two}^{analyt} (red) and I^{num} (black). The rest of parameters are: $n_y = 5$, $Q_x = 0.31$, $Q_y = 0.32$. The invariant is destroyed at $\approx 15\sigma$.

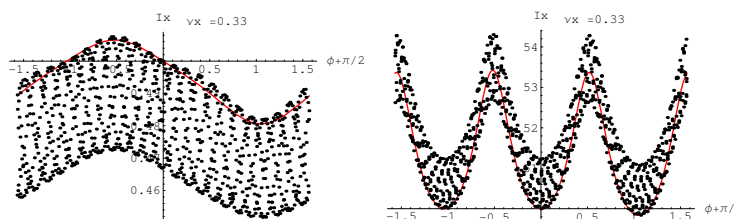


Figure 8: Near $1/3$ resonance. Left: $n_x = 1$; Right $n_x = 10$, both for $n_y = 1$ and $Q_x = 0.33$, $Q_y = 0.34$. The invariant is destroyed at $\approx 5\sigma$. [get eps](#)
[get eps](#)

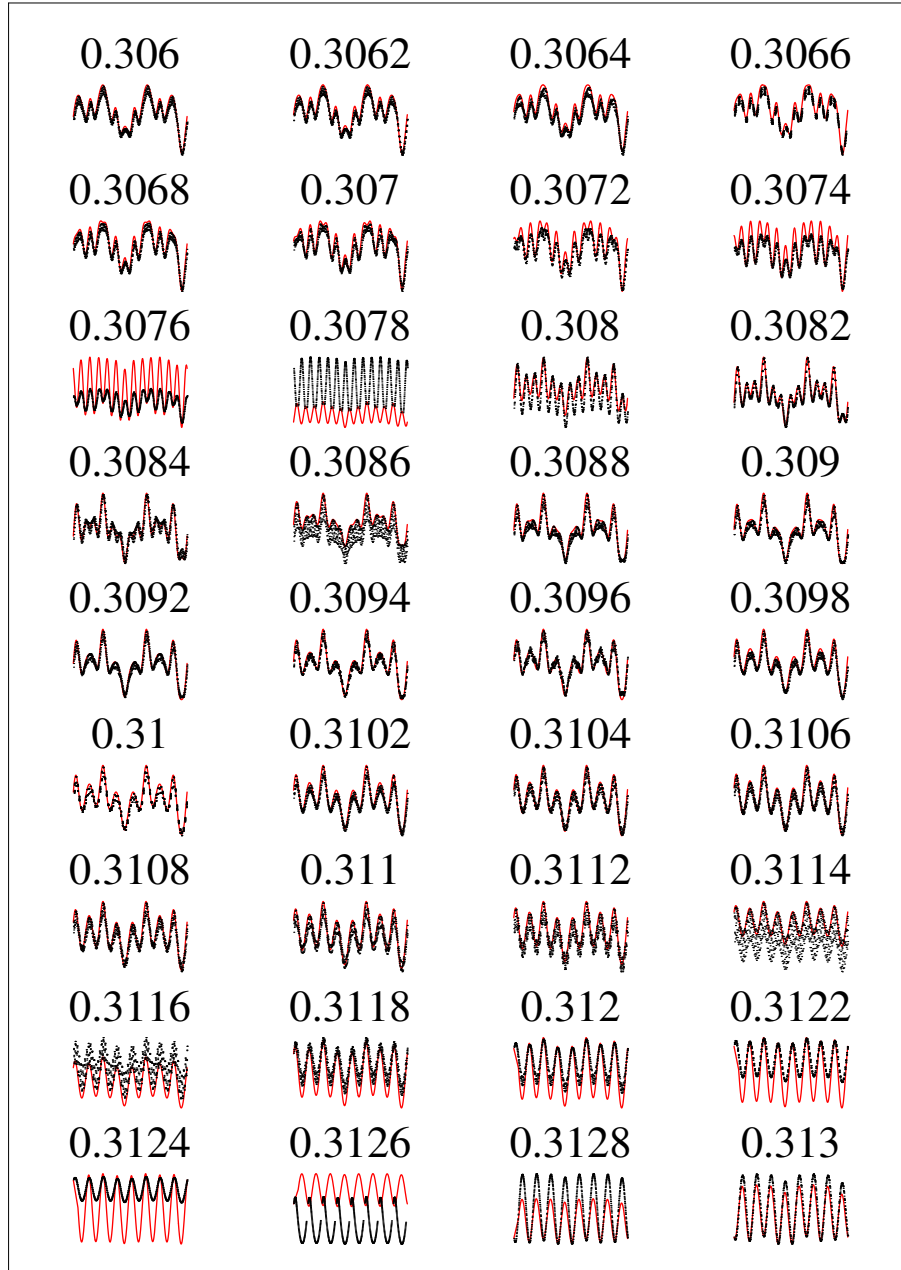


Figure 9: A tune-scan to detect the resonances at $\nu_x = 4/13 = 0.3077$ and $n\nu_x = 5/16 = 0.3125$. Shown are the value of ν_x ($\nu_y = \nu_x + .01$), the invariant (red) and the tracking points (black). The particle starts with: $n_x = 14$, $n_y = 1$. The second IP is at $\nu_{x,IP5} = 0.2604$, $\nu_{y,IP5} = 0.31/2$. [get eps](#)

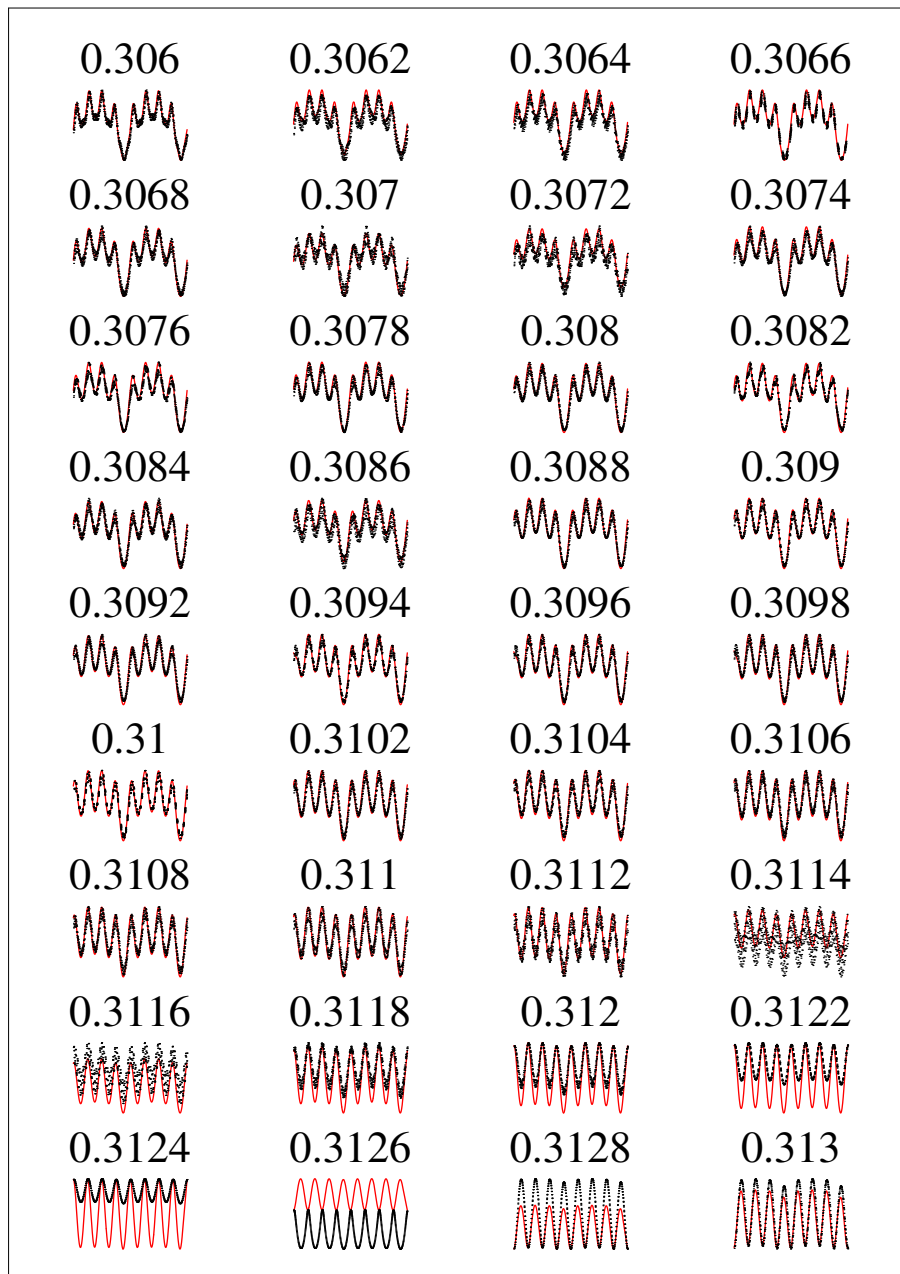


Figure 10: Here $\nu_{x,IP5} = 0.25$ and all other parameters are as on Figure 9 – to show that the first resonance (at $Q_x = 4/13 = 0.3077$) is absent. [get eps](#)